



Optimization of batch process parameters for Congo red color removal by *Neurospora crassa* live fungal biomass with wheat bran dual adsorbent using response surface methodology

P. Vairavel^a, V. Ramachandra Murty^{b,*}

^aDepartment of Chemical Engineering, Manipal Institute of Technology, Manipal Academy of Higher Education, Manipal, Karnataka state, India, Tel. +919036270978, email: pvairavel@gmail.com (P. Vairavel)

^bDepartment of Biotechnology, Manipal Institute of Technology, Manipal Academy of Higher Education, Manipal, Karnataka state, India, Tel. +91 9448529691, email: murty.vytla@manipal.edu (V.R. Murty)

Received 8 July 2017; Accepted 10 December 2017

ABSTRACT

The present work deals with the application of response surface methodology (RSM) to study the effects of various operational parameters on the decolorization of Congo red (CR) from dye wastewater. The live fungal biomass of *Neurospora crassa* along with wheat bran was used as a dual adsorbent for the removal of CR color from aqueous solution. Decolorization experiments were conducted in batch mode by varying experimental factors such as initial pH, initial dye concentration, wheat bran dosage, live biomass dosage, wheat bran particle size, and agitation speed. The process parameters were optimized using central composite design (CCD) to attain the maximum percentage decolorization. Predicted values of percentage color removal were found to be in good agreement with experimental values, which indicates that the suitability of the model and the success of CCD in optimization of CR color removal process. Graphical response surface and contour plots were used to locate the optimum points. The regression model equation for percentage CR color removal was established. The optimum pH, dye concentration, wheat bran dosage, live biomass dosage, wheat bran particle size and agitation speed were found to be 6, 200 mg L⁻¹, 12.5 g L⁻¹, 2% (w/v), 150 μm, 150 rpm, respectively for CR color removal. Further, the batch experiments were conducted to study the effect of electrolytes, surfactants, mixture of dyes, and temperature on dye decolorization. We concluded that the live fungal biomass of *Neurospora crassa* with wheat bran was shown to be suitable dual adsorbent for adsorption of CR and it can be used effectively in wastewater treatment.

Keywords: Congo red dye; *Neurospora crassa* live fungal biomass; Wheat bran; Color removal; Response surface methodology; Central composite design; Statistical analysis

1. Introduction

Dyes are ionic, synthetic origin and complex aromatic organic compounds which are extensively used in the textile, paper, printing, plastic, cosmetic, food, and pharmaceutical industries [1]. In textile industry, large amount of effluent is discharged from dyeing process whereby 10–15% of dyes are estimated to be lost in the effluent [2]. Worldwide, the total dye consumption of the textile industry is

in excess of 10⁷ kg/y [3]. However, approximately 1 million kg of textile dyes are discharged into industrial effluents every year [4]. Generally, color is visible in the effluents from textile-dyeing processes when the dye concentration is greater than 1 mg L⁻¹ and at an average concentration of 300 mg L⁻¹ [5]. The synthetic dye Congo red [1-naphthalene sulfonic acid, 3,3-(4,4-biphenylenebis(azo))bis (4-amino-) disodium salt] is a popular water soluble diazo anionic dye, which is known to metabolize benzidine, a human carcinogen [6]. It shows a high affinity for cellulose fibers and is

*Corresponding author.

used in textile processing industries. Azo dyes are highly toxic, mutagenic, carcinogenic and usually constitute health hazards [7]. CR has been known to cause an allergic dermatitis, skin, eye, and gastrointestinal irritation [3,8]. It is investigated as a mutagen and reproductive effector. It may affect blood factors such as clotting, and induce somnolence and respiratory problems [9]. Even a low concentration of CR dye causes various harmful effects such as difficulties in breathing, diarrhea, nausea, vomiting, abdominal and chest pain, severe headache, etc. [10]. Furthermore, dyes can significantly affect the dissolved oxygen concentration and photosynthetic activity in aquatic systems [11]. The effluents must be treated to bring down the concentration of dyes present in it to permissible and bearable limit before discharging into water bodies as required under environmental regulation act [8]. Therefore, the removal of CR from waste effluents is also of great environmental importance.

Many conventional methods such as chemical precipitation, ion exchange, membrane filtration, electrochemical oxidation, photo-catalytic degradation, ozonation, Fenton process, sonication, etc. have been widely used for the treatment of dyes bearing wastewater [12–14]. However, these technologies have several disadvantages such as high capital and operating cost, complexity of the treatment processes, sludge disposable problem, and the need of chemicals, which may in turn pollute the water [15,16]. Due to these limitations, there is a vital need for a more environmentally benign and cost-effective method. Furthermore, these methods cannot be used effectively to treat the wide range of dye wastewater [17]. Adsorption is a widely used technique as it provides an attractive alternative treatment, especially if the adsorbent is inexpensive and readily available. This process is becoming a superior and promising technology because of its simplicity, ease of operation and handling, insensitivity to toxic pollutants and sludge-free operation [13]. Additionally, this process is more eco-friendly because it does not result in the formation of harmful substances [3,13]. Optimized adsorption process have higher efficiency and adsorption capacity resulting in a high quality treated effluent. Adsorption on commercial activated carbon is the most popular adsorbent in many industries because of its excellent adsorption capacity and is used to remove various dyes from industrial effluents. However, activated carbon usage is limited due to high cost and its regeneration and reuse make it more costly [18]. However, in view of the high cost and associated problems of regeneration, there is a need for alternate low cost, easily available and more effective adsorbents [13]. These include agricultural by-products, such as pine tree leaves [19], cat-tail roots [20], sunflower stalks [21], castor seed shells [22], soy meal hull [23], wheat bran [24], etc., which have been used for removing color from dye wastewater.

In biological treatments, microbial decolorization of dye can be classified into two kinds according to their life state: For living cells, the major mechanism is biodegradation because they can produce lignin modifying enzymes such as, laccase, manganese peroxidase (MnP) and lignin peroxidase (LiP) to biodegrade/biotransform the synthetic dyes. For dead cells, the mechanism is biosorption, which involves physico-chemical interaction between adsorbate and adsorbent [14,25]. Various types of live fungal biomass such as *Phanerochate chrysosporium* [26], *Pleurotus ostreatus*

[27], *Rhizopus oryzae* [28], *Irpex lacteus* [29], *Funalia trogii* [30], among others, can be used to remove color from dye wastewater. The potential of using live biomass with wheat bran as effective dual adsorbent to remove azo dyes has not been explored. The dual adsorbent had better adsorption efficiency in the removal of color from dye wastewater when compared to the individual adsorbents and the process with dual adsorbent is rapid [31,32]. The literature survey indicates that color removal from dye effluents using live biomass with agricultural waste are limited. Decolorization of selected toxic dye compounds with few types of live fungal biomass and the use of agricultural by-product as a low-cost adsorbent of dye molecules have been studied. Therefore, the present paper focused an economical treatment process to remove the CR color from its aqueous solution using dual adsorbent consisting of live fungal biomass of *Neurospora crassa* and wheat bran. The effect of various parameters on CR color removal process were optimized using response surface methodology to achieve the best overall optimization of the dual adsorbent system. *Neurospora crassa* (the common pink bread mould) is a filamentous non-pathogenic ascomycete fungus and ease of growth in nutrient (broth) medium [33,34]. Wheat bran is the outer shell of wheat grain, and an agricultural by-product of the wheat milling operation; furthermore, wheat bran is an economically viable and most readily available natural material in India.

2. Materials and methods

2.1. Preparation various adsorbent (agricultural by-product)

Various agricultural by-products such as rice husk, wheat straw, sugarcane bagasse, coir pith and saw dust were collected locally in Udupi District, Karnataka state, India. Wheat bran and rice bran were procured from M/s Ganesh flourmill industries, Kolkata, India. The above materials were dried under sunlight to remove the moisture and ground to fine powder using pulverizer. The materials were washed with distilled water to remove all the dirt particles. Then, the materials were dried in a hot-air oven at the temperature of 333 K for 24 h, ground, and screened to obtain particles < 100 μm in size [35]. Various materials were then stored in different airtight plastic bottles for further use.

2.2. Preparation of *Neurospora crassa* live fungal biomass

The filamentous fungus *Neurospora crassa* (MTCC 1852) used in this study was obtained from the Institute of Microbial Technology, Chandigarh, India, and was stored at 277 K. A loopful of inoculum (stock culture of the organism) was streaked on potato dextrose agar plates and it was grown at 298 K for 4 days, and plates were maintained at 277 K until use. New culture plates were prepared every 25 days. The potato dextrose broth medium of 100 mL was inoculated with the live fungal culture in Erlenmeyer flasks (base diameter of the flask = 7.5 cm) under sterile conditions. The fungi were allowed to grow (submerged cultivation) for one week in a shake flask in an incubator shaker rotated at a speed of 120 rpm at 298 K to get maximum amount of fungal biomass [33,34]. After sufficient growth, the live fun-

gal biomass was filtered to remove from the liquid medium using Whatman filter paper (grade 41).

2.3. Pre-treatment of glassware

Dyes can strongly adsorb on the glass. To minimize this effect, all glassware to be used in contact with dye solutions were steeped before use for 24 h in a solution (1000 mg L⁻¹) of a cationic surface-active agent, cetyltrimethylammonium bromide (CTAB), which is preferentially adsorbed. The glass surfaces were then thoroughly rinsed with water before use [36].

2.4. Chemicals required

An anionic dye Congo red (Dye content ≥35%, Molecular formula = C₃₂H₂₂N₆Na₂O₆S₂, Molecular weight = 696.66, λ_{max} = 498 nm) supplied by Sigma Aldrich, India was used in the study. The dye was of analytical reagent grade, and of 99.8% purity. The other anionic dyes like Coomassie violet, Remazol brilliant blue, and Acid green 25 were also obtained from Sigma Aldrich, India. The analytical grade potato dextrose agar and potato dextrose broth were obtained from Himedia, India. All other chemicals used were of analytical grade (Merck, India).

2.5. Preparation of CR dye stock solution

A stock solution of 1000 mg L⁻¹ was prepared by dissolving accurate quantity of CR dye powder in distilled water. The experimental solution of required initial dye concentration was obtained by diluting the stock solution with pH adjusted distilled water by adding 0.1 N HCl or 0.1 N NaOH. After dilution (adjusting the pH), the required pH of the dye solution was measured.

2.6. Analytical measurements

The pH of the dye solution was observed by a digital pH-meter (Systronics 335). The surface area and pore volume of the wheat bran were determined using a Brunauer–Emmett–Teller (BET) surface analyzer (Smart Instruments, India). The average particle size of the wheat bran was evaluated by a particle size analyzer (Cilas 1064, France). A double-beam UV/visible spectrophotometer (Shimadzu UV-1800) was used to determine the unknown residual concentration of CR dye solution.

2.7. Batch adsorption studies

The required amount of live fungal biomass and wheat bran were added to the CR dye aqueous solution to initiate the decolorization experiments. Batch experiments were conducted by varying the level of one factor and keeping the level of other factors constant on the other hand. Adsorption studies were carried out at 303 K to examine the effect of initial pH, initial dye concentration, wheat bran dosage, live biomass dosage, wheat bran particle size, and agitation speed on the removal of CR color from aqueous solution using live biomass-wheat bran (LB-WB) dual

adsorbent. Furthermore, the experiments were conducted to study the effect of electrolytes, surfactants and temperature on dye decolorization in batch mode. The experiments were conducted by stirring CR dye aqueous solution at 150 rpm for 10 h at 303 K with required initial dye concentration in each flask containing fixed quantity of live biomass and wheat bran dosage. A known amount of solution was withdrawn at regular time intervals. Then, the samples were centrifuged (Remi CPR-24 Plus) at 12000 rpm for 10 min to settle down the suspended particles [3]. After centrifugation, the clear supernatant liquid was obtained and analyzed for the residual dye concentration. The percentage CR color removal was determined by the following Eq. (1) [37]:

$$\% \text{ CR color removal} = \frac{(C_o - C_t) \times 100}{C_o} \quad (1)$$

where C_o and C_t (mg L⁻¹) are the liquid-phase concentrations of CR at initial and time t, respectively. Decolorization (adsorption) experiments were conducted at 10 h. The microbial growth and enzyme activity of the samples were not analyzed during the process.

2.8. Experimental design and optimization of process parameters

The experimental design was constructed through Minitab 16 statistical software and CCD was applied to conduct decolorization experiments. CCD consist of a factorial design with centre points, augmented with a group of axial (or star) points that allow the estimation of curvature to fit the quadratic model [38]. The influencing factors such as initial pH (X₁), initial dye concentration (X₂), wheat bran dosage (X₃), live biomass dosage (X₄), wheat bran particle size (X₅), and agitation speed (X₆) were chosen as the independent variables while the percentage color removal was set as the response (dependent) variable. The required experimental runs are calculated using the following Eq. (2) [39]:

$$N = 2^f + 2f + N_o \quad (2)$$

while, f represents the number of variables, 2^f represent the number of factorial points, 2f represents the axial points and the center points are represented by N_o. A total of 53 experiments were conducted including 32 cube points, 12 axial points, and 9 center points using 2⁶ half factorial design. The repetition of central point gives an estimated error. The levels of independent variables were coded as -2 (very low), -1 (low), 0 (central point), 1 (high), and 2 (very high). The coded values of process variables were obtained from Eq. (3) [40]:

$$x_i = \frac{(X_i - X_o)}{\delta X} \quad (3)$$

where x_i is the dimensionless value of a process variable; X_i is the real value of an independent variable; X_o is the value of X_i at the center point and δX denotes the step change. The polynomial expression for the relation between the independent and response variables is given as [40]:

$$Y = \beta_0 + \sum \beta_i x_i + \sum \beta_{ii} x_i^2 + \sum \beta_{ij} x_i x_j \quad (4)$$

where Y is the predicted response variable of percentage decolorization; β_0 is the offset term; and β_i , β_{ii} , and β_{ij} are the regression coefficients for linear, quadratic, and interaction effects, respectively. Analysis of variance (ANOVA) is a statistical technique that is widely employed to assess the significance of various variables in the decolorization process. Both value and sign in ANOVA table are important for the regression coefficients. The positive sign increases the response, while the negative sign decreases the response. These analyses were done by means of main effects, interaction effects, coefficients of the model, standard deviation of each coefficient, probability level, Fisher's 'F'-test, and Student 'T'-test. The probability level, P , was used to verify the significance of each of the interactions among the factors and T-tests were applied to evaluate the significance of the regression coefficients of the parameters. Larger magnitude of T and lower values of P ($P < 0.05$) indicates that the linear, quadratic, and interaction effects are more significant in the chosen model at the corresponding coefficient terms. The suitability of the response surface model was assessed by the values of regression coefficient (R^2), coefficient of variation, adequate precision and by the analysis of lack of fit. The value of R^2 between zero and one ($0 < R^2 < 1$) and the larger value was better. The central point carried out in duplicate was useful to obtain the standard error of the coefficients [40–42]. The significant factors are arranged in ascending order with respect to their significance and hence the most significant factor is determined easily.

2.8.1 Residuals analysis

The predicted responses obtained from RSM were compared to the actual responses, for verification of the predicted data. The root mean squares error (RMSE) and the absolute average deviation (AAD) are used to predict the adequate precision of the model equation. The RMSE and AAD were determined using Eqs. (5) and (6), respectively [41].

$$\text{RMSE} = \sqrt{\left(\frac{1}{N} \sum (y_a - y_p)^2 \right)} \quad (5)$$

$$\text{AAD} = \frac{1}{N} \sum \left(\frac{y_p - y_a}{y_a} \right) \times 100 \quad (6)$$

where y_a is the actual response value, y_p is the predicted response value obtained from the RSM, and N is the number of experiments.

3. Results and discussion

3.1. Selection of suitable agricultural by-product

Adsorption experiments were performed using various agricultural by-products such as rice husk, wheat straw, sugarcane bagasse, coir pith, saw dust, wheat bran and rice bran at room temperature to evaluate the maximum percentage of CR color removal and the results were shown

in Fig. S1 of supplementary materials. It showed that maximum decolorization of CR was observed in the adsorbent wheat bran. The maximum percentage color removal using wheat bran was 82.05% at pH 6. It may be due to availability of more number of active sites in the wheat bran surface. Therefore, out of seven different adsorbent options, wheat bran was found to exhibit better results and was studied for further analysis.

3.2. Characterization of the adsorbent

The BET surface area of the wheat bran was $1.93 \text{ m}^2 \text{ g}^{-1}$. The pore volume of the wheat bran was found to be $1.64 \text{ mm}^3 \text{ g}^{-1}$ with the average particle size of $61.50 \text{ }\mu\text{m}$. The active sites present in wheat bran surface area with live fungal biomass are responsible for CR dye uptake.

3.3. Analysis of various parameters in batch adsorption studies

Adsorption experiments were conducted at 10 h. The intensity of the peaks of synthetic CR dye effluent was measured before and after treatment. During this 10 h, the peak wavelength (λ_{max}) of treated synthetic CR dye effluent was similar to original untreated CR dye wavelength of concentration 200 mg L^{-1} . The intensity of the peaks reclined considerably after treatment which indicates that CR dye molecules were adsorbed on LB-WB dual adsorbent in 10 h (Fig. S2 of supplementary materials). Therefore, absorbance values of all the experiments were measured at 498 nm before and after treatment in 10 h.

3.3.1. Effect of initial pH

To analyze the effect of the initial pH on CR dye decolorization under a strongly acidic pH was difficult because of the formation of protonated species, which may lead to a change in the structure of the dye. The CR dye in aqueous solution was black in color at acidic pH (<5), due to the formation of a quinonoid structure [31,43]. The red color remained stable in the pH range of 6–12, and it becomes unstable if the solution pH decreased less than 6. The color of CR in aqueous solutions is strongly pH-dependent due to its structure transformation [31]. Therefore, the effect of initial pH on color removal from aqueous solution was analyzed between pH 6–12.

As shown in Fig. 1, the decolorization of CR was found to decrease from 97.27 to 55.68% with the increase in pH from 6–12. More than 80% color removal is observed in the pH range of 6–9. The maximum decolorization of CR was observed at pH 6. Therefore, further decolorization experiments were carried out at pH 6. At pH 6, the surface of LB-WB dual adsorbent gets positively charged and adsorbs the negatively charged dye anions through significant electrostatic forces of attraction. So, the decrease in CR removal with increasing pH, in the present study, can be attributed to decrease in electrostatic attractions between active sites in the dual adsorbent and CR dye molecules. As the pH of the system increases, the number of negatively charged sites increases and the number of positively charged sites decreases. A negatively charged surface sites on the LB-WB dual adsorbent does not favor the decolorization of dye

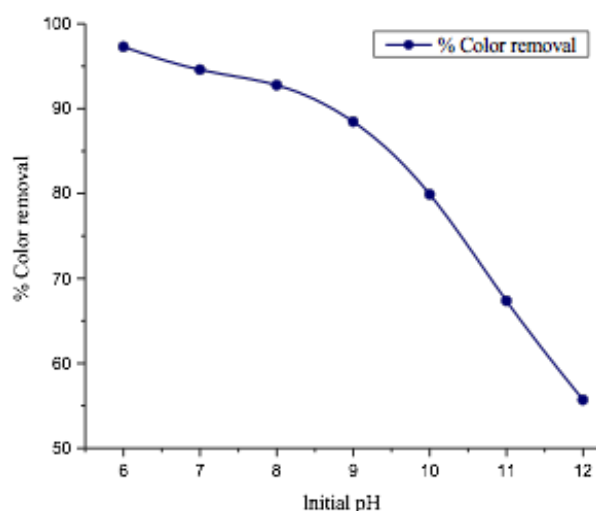


Fig. 1. Effect of initial pH on CR color removal by LB-WB dual adsorbent.

(Initial dye concentration: 200 mg L^{-1} ; wheat bran dosage: 10 g L^{-1} ; live biomass dosage: 1.5% (w/v); wheat bran particle size: $<100 \mu\text{m}$; agitation speed: 150 rpm; temperature: 303 K; contact time 10 h).

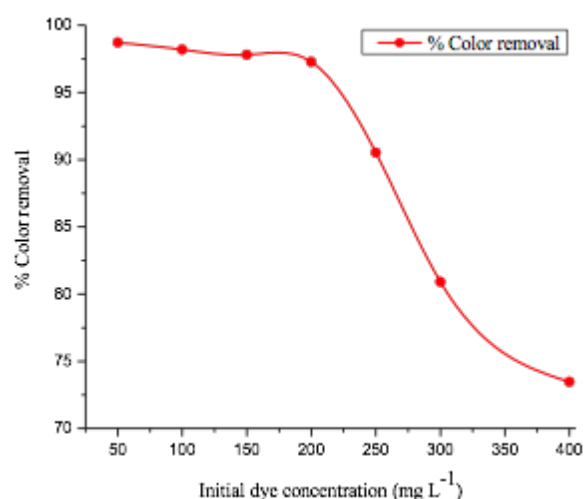


Fig. 2. Effect of initial dye concentration on CR color removal by LB-WB dual adsorbent.

(Initial pH: 6; wheat bran dosage: 10 g L^{-1} ; live biomass dosage: 1.5% (w/v); wheat bran particle size: $<100 \mu\text{m}$; agitation speed: 150 rpm; temperature: 303 K; contact time 10 h).

anions due to the electrostatic repulsion. Also, lower percentage decolorization of CR observed at basic pH may be due to competition between the excess hydroxyl ions and the negatively charged dye ions for the available adsorption active sites [44].

3.3.2. Effect of initial dye concentration

The influence of CR dye concentration on color removal was analysed by varying the initial dye concentration from 50 to 400 mg L^{-1} . The percentage color removal of CR decreased from 98.71 to 73.46% with the increase in dye concentration (Fig. 2). This is due to accumulation of dye molecules in the available binding sites and competition between more dye anions at the positive charge of fixed binding sites of the LB-WB dual adsorbent. The percentage color removal declined gradually upto 200 mg L^{-1} , however, drops drastically above 200 mg L^{-1} . As the initial dye concentration was increased, the vacant sites on the surface of the dual adsorbent were saturated (i.e., enhances the interaction between dye molecules and active sites on the dual adsorbent surface, therefore, lack of available active sites), leading to the decrease of the percentage decolorization [45].

3.3.3 Effect of wheat bran and live biomass dosage

The effect of wheat bran dosage on color removal was analyzed by varying the wheat bran dosage from 0.25–1.75 g per 100 mL of dye solution with an initial dye concentration of 300 mg L^{-1} at pH 6. From the Fig. S3 of supplementary materials, it can be seen that the decolorization efficiency of CR increased from 64.90 to 90.34% with the increase in the wheat bran dosage. The increase in the percentage color removal with the wheat bran dosage can be attributed to the availability of greater surface area resulted in the increase

in the availability of adsorption active sites. Similarly, the effect of live biomass dosage was studied by varying the dosage from 0.5 to 3% (wet % by w/v). The increase in live biomass dosage increased the color removal percentage from 81.33 to 91.74% (Fig. S4 of supplementary materials). This may be due to availability of more adsorption active sites at higher concentrations of the adsorbent for the removal of CR dye. Thus the competition for the availability of active sites for the adsorption of dye decreases with the increase in the adsorbent dosage. In other words, at higher adsorbent (wheat bran/live biomass)-to-dye concentration ratios, adsorption onto the dual adsorbent surface is very rapid, thus producing a lower dye concentration in the solution, compared to that obtained for a lower dual adsorbent-to-dye concentration ratio [35]. Therefore, increase in adsorbent dosage resulted in a decrease in the dye concentration in the solution.

3.3.4. Effect of wheat bran particle size

The influence of wheat bran particle size on color removal was studied by varying the wheat bran particle size from 100 to $600 \mu\text{m}$. The results show that the decolorization efficiency was dependent on the particle size. There was a gradual increase of percentage decolorization with the decrease in particle size. From the Fig. S5 of supplementary materials, the decolorization of CR decreased gradually from 90.55 to 70.92% with an increase in wheat bran particle size from 100 to $600 \mu\text{m}$. The higher percentage color removal with smaller particle size may be attributed to the fact that the small particles provided a larger surface area per unit mass [24]. Also, the smaller particles will have a shorter diffusion path, thus allowing the dye molecules to penetrate deeper into the wheat bran particles quickly, resulting in a higher percentage adsorption [40].

3.3.5. Effect of agitation speed

The effect of agitation speed in a batch process is important to overcome the external mass transfer resistance. Influence of agitation speed on color removal was evaluated by varying the agitation speed from 0 to 250 rpm (250 rpm = 25.51 g; base diameter of the Erlenmeyer flask = 7.5 cm, volume = 250 mL). Fig. S6 of supplementary materials illustrates that the CR color removal increased from 36.24 to 94.36% with increasing agitation speed. The increase in removal efficiency may be due to increase in turbulence attributable to decrease in the film boundary layer thickness (film resistance) surrounding the dual adsorbent, thus increasing external film diffusion and uptake of CR dye molecules [46]. This phenomenon may be explained by increasing the contact surface of dual adsorbent-dye solution and favouring the transfer of dye molecules to the dual adsorbent active sites [47].

3.3.6. Effect of temperature

Textile effluents are released at relatively high temperature (323–333 K); so temperature will be an important parameter affecting the color removal efficiency in the real application of adsorption by LB-WB dual adsorbent. The effect of temperature on color removal was analyzed by varying the temperature from 303 to 333 K and the results are shown in Fig. 3. From this figure it shows that the decolorization of CR increased from 90.56 to 98.24% with increasing temperature. However, maximum color removal was obtained at a temperature of 333 K. This phenomenon may be due to an increase in the mobility of CR dye molecules across the boundary layer with increasing temperature. An increasing number of dye molecules may also acquire sufficient energy to undergo an interaction with active sites at the dual adsorbent surface [48]. The enhancement of percentage color removal might be due to chemical interaction

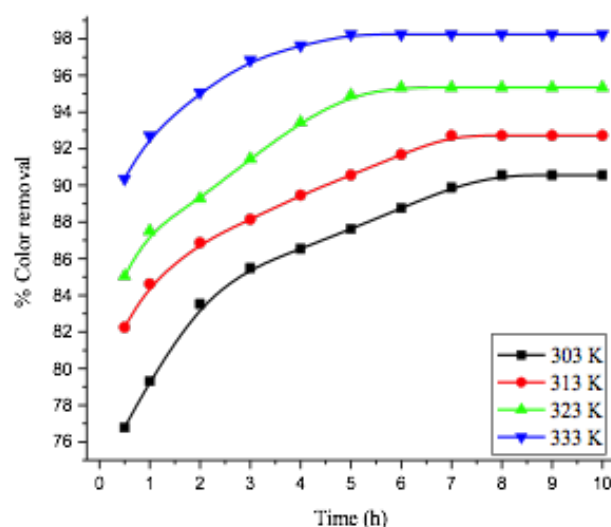


Fig. 3. Effect of temperature on CR color removal by LB-WB dual adsorbent.

(Initial pH: 6; initial dye concentration: 300 mg L⁻¹; wheat bran dosage: 12.5 g L⁻¹; live biomass dosage: 2% (w/v); wheat bran particle size: <100 μm; agitation speed: 150 rpm; contact time 10 h).

between adsorbate and adsorbent, creation of some new adsorption active sites or the increased rate of intraparticle diffusion of CR dye molecules into the pores of the adsorbent (wheat bran) at higher temperatures [49,31]. Furthermore, increasing temperature may produce a swelling effect within the internal structure of the wheat bran enabling more dye molecules to penetrate further [48].

3.4. Interruption of other parameters on CR dye decolorization

3.4.1. Effect of electrolytes

Dyeing processes consume large amounts of dissolved inorganic salts. The presence of salt concentration in the industrial effluent (ionic strength of the solution) is one of the important factors which influence the decolorization efficiency [50]. Therefore, sodium chloride (NaCl), sodium bicarbonate (NaHCO₃), sodium nitrate (NaNO₃), calcium chloride (CaCl₂), and magnesium chloride (MgCl₂) were chosen as model inorganic salts [51]. The concentrations of the electrolytes were varied from 0 to 1.5% (w/v) and the results were plotted in Fig. 4. The results suggested that the percentage colour removal for various electrolytes gradually increased with increase in their concentration. Theoretically, when the electrostatic forces between the adsorbent surface and electrolytes were attractive, there will be a decrease in the percentage decolorization of CR dye. Conversely, when the electrostatic attraction is repulsive, an increase in ionic strength will increase the percentage color removal of CR dye. The increase in color removal at high concentration of electrolyte was caused by increase in dimerization of dye molecules in solution [52]. A number of intermolecular forces such as van der Waals forces; ion-dipole forces; and dipole-dipole forces have been suggested to explain this

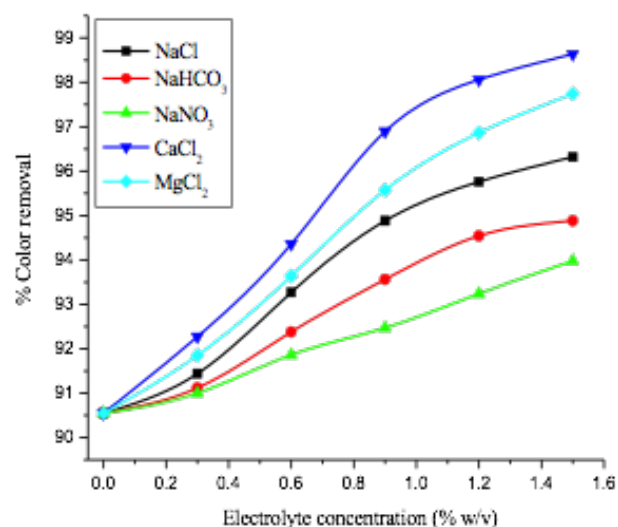


Fig. 4. Effect of electrolytes on CR color removal by LB-WB dual adsorbent.

(Initial pH: 6; initial dye concentration: 300 mg L⁻¹; wheat bran dosage: 12.5 g L⁻¹; live biomass dosage: 2% (w/v); wheat bran particle size: <100 μm; agitation speed: 150 rpm; temperature: 303 K; contact time 10 h).

aggregation. These forces which occur between dye molecules and it may be increased upon the addition of salt to the dye solutions [53]. Generally salt ions, forces the dye molecules to aggregate and enhancing the extent of percentage color removal. Hence the studied adsorption processes holds good even with the presence of considerable quantity of the electrolytes. A similar observation has been reported elsewhere [16,52].

3.4.2. Effect of surfactants

Surfactants are generally used in textile dyeing process and thus may be present in industrial effluent. The effect of various surfactants such as CTAB (cationic surfactant), sodium dodecylbenzene sulfonate (SDS, anionic surfactant), Polysorbate-80 (Tween-80, non-ionic surfactant), and polyoxyethyleneglycol t-octylphenyl ether (Triton X-100, non-ionic surfactant) were carried on the decolorization process at optimized conditions. The effect of surfactant on color removal was studied by varying the surfactant concentration from 0 to 1.5% (w/v) for CTAB, SDS and from 0 to 2% (v/v) for non-ionic surfactants. The experiments were carried out for 10 h and the results were shown in Figs. 5 and 6. It was revealed from Fig. 5 that non-ionic surfactants slightly increased the decolorization of CR from 90.56 to 96.22% for Tween-80 and from 90.56 to 94.79% for Triton X-100 respectively. This may be due to electrostatic forces between the dual adsorbent surface and surfactants were repulsive [52]. The ionic surfactants CTAB and SDS reduce the decolorization of CR to 38.62% and 19.88% respectively (Fig. 6). This phenomenon may be explained by the existence of barrier energy between the ionic surfactants and dye molecules or dual adsorbent. A similar observation has been reported elsewhere [16].

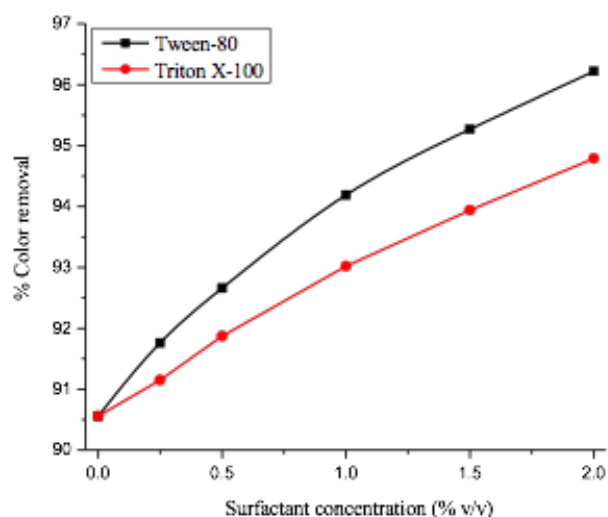


Fig. 5. Effect of non-ionic surfactants on CR color removal by LB-WB dual adsorbent.

(Initial pH: 6; initial dye concentration: 300 mg L⁻¹; wheat bran dosage: 12.5 g L⁻¹; live biomass dosage: 2% (w/v); wheat bran particle size: <100 μm; agitation speed: 150 rpm; temperature: 303 K; contact time 10 h).

3.4.3. Effect of mixture of dyes

The optimal values of various experimental factors which is obtained from batch studies and CCD were used to remove COD from mixture of dyes such as Congo red (CR), Coomassie violet (CV), Remazol brilliant blue R (RBBR), and Acid green 25 (AG 25). The effect of mixture of dyes on COD removal was studied by contacting 100 mL mixture of above dyes of various concentration from 50 to 400 mg L⁻¹ at room temperature (303 K). The other experimental factors were kept constant. The COD removal of mixture of dyes decreased from 87.13 to 60.18% with increase in initial concentration of mixture of dyes as shown in Fig. 7. As the initial dye concentration was increased, the available binding sites on the surface dual adsorbent were saturated, leading to the decrease of percentage COD removal. The intensity of the peaks of mixture of dye solution was measured before and after decolorization. The intensity of peaks declined considerably after treatment using LB-WB dual adsorbent (Fig. 8). Therefore, live fungal biomass-wheat bran dual adsorbent was effectively used to decrease the pollutant level from mixture of dyes in aqueous solution.

3.5. Analysis of factorial experimental design and optimization of process parameters (Analysis of variance)

The important factors depends on decolorization were initial pH, initial dye concentration, wheat bran dosage, live biomass dosage, wheat bran particle size, and agitation speed. Various groups of independent variables were used to study the mutual effect of different parameters using statistically designed experiments. The experimental ranges and levels of various independent variables in CR color removal are given in Table 1. The comparison of predicted response values with experimental results is reported in Table 2. The results were analyzed by ANOVA and are

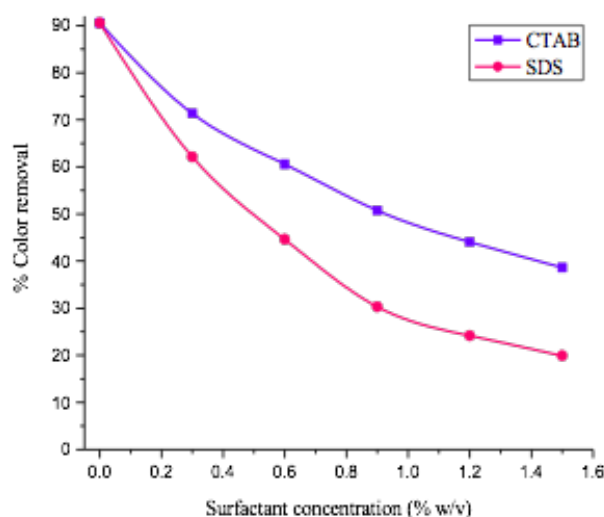


Fig. 6. Effect of ionic surfactants on CR color removal by LB-WB dual adsorbent.

(Initial pH: 6; initial dye concentration: 300 mg L⁻¹; wheat bran dosage: 12.5 g L⁻¹; live biomass dosage: 2% (w/v); wheat bran particle size: <100 μm; agitation speed: 150 rpm; temperature: 303 K; contact time 10 h).

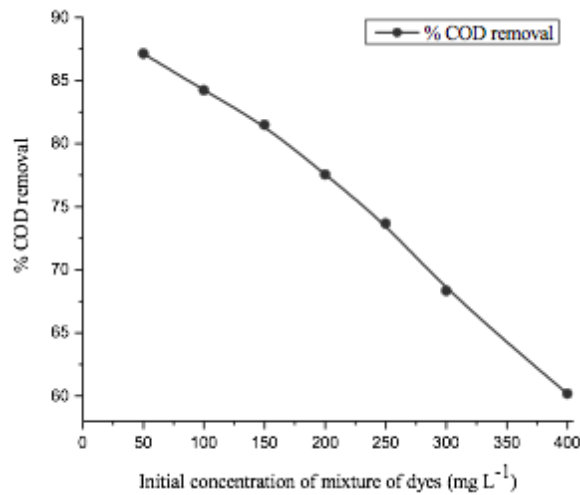


Fig. 7. Effect of initial dye concentration on mixture of dyes by LB-WB dual adsorbent. (Initial pH: 6; wheat bran dosage: 12.5 g L⁻¹; live biomass dosage: 2% (w/v); wheat bran particle size: <100 μm; agitation speed: 150 rpm; temperature: 303 K; contact time 10 h).

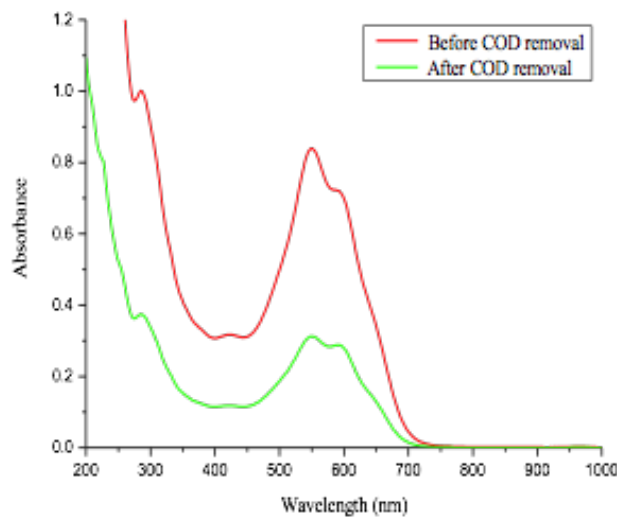


Fig. 8. Profile of synthetic dye effluent mixture before and after COD removal. (Initial pH: 6; initial dye mixture concentration: 100 mg L⁻¹; wheat bran dosage: 12.5 g L⁻¹; live biomass dosage: 2% (w/v); wheat bran particle size: <100 μm; agitation speed: 150 rpm; temperature: 303 K; contact time 10 h).

given in Table 3. The coefficients for the linear effect of initial pH, initial dye concentration (X_2), wheat bran dosage, live biomass dosage, and agitation speed were the primary significant factors ($P = 0.000$). Wheat bran particle size was the second important factor ($P = 0.017$). The coefficients for the linear effect of all the factors were highly significant on the effect of decolorization of CR by LB-WB dual adsorbent. The coefficients of the quadratic effect of all the variables ($X_1, X_2, X_3, X_4, X_5, X_6$) are not significant. The coefficient of the interaction effect between initial pH (X_1) and initial dye

Table 1

Experimental range and levels of independent variables for CR color removal by live biomass with wheat bran dual adsorbent

Independent variables	Range and level				
	-2	-1	0	1	2
Initial pH (X_1)	5.6	5.8	6.0	6.2	6.4
Initial dye concentration, mg L ⁻¹ (X_2)	200	250	300	350	400
Wheat bran dosage, g (X_3)	0.75	1.0	1.25	1.5	1.75
Live biomass dosage, % w/v (X_4)	1	1.5	2	2.5	3
Wheat bran particle size, μm (X_5)	100	125	150	175	200
Agitation speed, rpm (X_6)	90	120	150	180	210

concentration (X_2) was the first important factor ($P = 0.000$). The coefficients of the interaction effect between X_2X_4 and X_4X_5 were the second and third important factors respectively ($P = 0.009, P = 0.017$). However, the coefficients of the other interactive effects among the variables did not appear to be very significant. The linear effect of X_3, X_4, X_6 and quadratic effect X_1, X_4 have positive effects on response. Similarly, the interaction effect between $X_1X_3, X_2X_4, X_3X_4, X_3X_5, X_4X_5, X_4X_6$ have positive effects and others have negative effects on response. The larger value of $F_{statistics}$ indicates that most of the variation in the response can be explained by the regression model equation [40]. According to the results, an empirical relation between independent variables and the response was gained and stated in the following second-order polynomial Eq. (7):

$$\begin{aligned} \% \text{ CR removal} = & 88.7806 - 1.5126 X_1 - 4.4222 X_2 + 1.0046 X_3 \\ & + 1.5811 X_4 - 0.6175 X_5 + 1.2256 X_6 + 0.0522 X_1^2 - 0.3897 X_2^2 \\ & - 0.1104 X_3^2 + 0.0407 X_4^2 - 0.1794 X_5^2 - 0.1970 X_6^2 - 1.1447 X_1 X_2 \\ & + 0.1653 X_1 X_3 - 0.0347 X_1 X_4 - 0.2172 X_1 X_5 - 0.3228 X_1 X_6 \\ & - 0.3591 X_2 X_3 + 0.7909 X_2 X_4 - 0.4841 X_2 X_5 - 0.3759 X_2 X_6 \\ & + 0.2172 X_3 X_4 + 0.3972 X_3 X_5 - 0.2434 X_3 X_6 + 0.7222 X_4 X_5 \\ & + 0.0166 X_4 X_6 - 0.1084 X_5 X_6 \end{aligned} \quad (7)$$

The regression coefficient, R^2 quantitatively evaluates the correlation between the experimental data and the predicted responses. The coefficient of variation shows the unexplained changes in the data, based on a percent of the response variable mean. The predicted response values match the experimental data's reasonably well with R^2 of 0.9537, which indicates that 95.37% of the variations in response could be described by this model and this also means that the model does not explain only about 4.63% of the variation. Adjusted R^2 (0.9037) is a tool to measure the goodness of fit, but it is more suitable for comparing models with various operating parameters. It corrects the R^2 value for the number of terms in the model and the sample size by using the degrees of freedom in its computations. Predicted R^2 (0.7055) can prevent overfitting the model and can be calculated from predicted residual error sum of squares (PRESS) statistics. Larger values of predicted R^2 suggest models of greater predictive ability. This may indicate that

Table 2
Six factor half factorial central composite design matrix for CR color removal by LB-WB dual adsorbent

Run no.	X_1	X_2 (mg L ⁻¹)	X_3 (g)	X_4 (% w/v)	X_5 (μm)	X_6 (rpm)	Decolorization efficiency (%)	
							Experiment	Predicted
1	1	1	1	-1	1	-1	77.98	77.37
2	0	0	0	0	0	0	88.79	88.78
3	1	1	1	-1	-1	1	81.62	81.19
4	1	1	1	1	1	1	84.55	84.28
5	0	0	0	0	0	0	88.78	88.78
6	-1	-1	1	-1	1	-1	90.72	91.15
7	0	0	0	0	0	0	88.94	88.78
8	-1	-1	-1	-1	-1	-1	89.26	89.76
9	0	0	0	0	0	0	88.60	88.78
10	0	0	-2	0	0	0	85.48	85.77
11	1	1	-1	-1	1	1	75.46	76.19
12	0	0	0	0	-2	0	90.24	89.23
13	0	0	0	0	0	0	88.79	88.78
14	-1	-1	-1	-1	1	1	91.45	91.99
15	-1	1	-1	1	1	1	89.38	88.71
16	1	-1	1	-1	-1	-1	91.26	92.16
17	-1	1	1	1	1	-1	89.62	88.73
18	-1	-1	1	1	-1	-1	92.53	92.02
19	0	0	0	0	0	0	89.14	88.78
20	0	0	0	2	0	0	93.78	92.77
21	-1	1	-1	-1	-1	1	86.85	87.07
22	0	0	0	0	0	-2	82.78	84.75
23	0	0	0	-2	0	0	84.87	85.25
24	1	1	-1	1	1	-1	80.51	80.55
25	1	-1	-1	1	-1	-1	90.44	89.44
26	0	0	0	0	0	0	88.62	88.78
27	-1	-1	1	-1	-1	1	94.78	94.96
28	0	0	2	0	0	0	91.46	90.55
29	0	-2	0	0	0	0	97.45	97.09
30	1	-1	-1	1	1	1	92.13	92.47
31	0	0	0	0	0	0	88.58	88.78
32	-1	-1	-1	1	-1	1	93.25	94.08
33	-2	0	0	0	0	0	95.82	92.67
34	1	1	1	1	-1	-1	84.39	84.07
35	-1	1	-1	1	-1	-1	85.94	86.96
36	1	-1	1	1	1	-1	94.38	94.38
37	-1	1	-1	-1	1	-1	79.81	80.27
38	1	-1	1	1	-1	1	95.18	94.94
39	1	-1	1	-1	1	1	93.64	92.84
40	1	-1	-1	-1	-1	1	91.96	93.07
41	-1	-1	1	1	1	1	96.12	97.82
42	0	0	0	0	0	2	93.18	90.58
43	-1	1	1	-1	-1	-1	84.39	84.28
44	-1	1	1	1	-1	1	87.20	90.16
45	0	2	0	0	0	0	76.33	76.06
46	0	0	0	0	2	0	85.92	86.30
47	1	1	-1	-1	-1	-1	81.04	79.56
48	-1	1	1	-1	1	1	82.46	83.68
49	0	0	0	0	0	0	88.57	88.78
50	1	1	-1	1	-1	1	84.32	84.12
51	2	0	0	0	0	0	82.96	85.48
52	-1	-1	-1	1	1	-1	89.88	90.53
53	1	-1	-1	-1	1	-1	89.85	87.12

Table 3

ANOVA for percentage CR color removal using live biomass with wheat bran dual adsorbent from the data of CCD experiments

Term	Coefficient	SE of coefficient	T _{statistics}	DF	Seq SS	Adj SS	Adj MS	F _{statistics}	Probability
Constant	88.7806	0.5292	167.778						
Regression				27	1302.32	1302.32	48.234	19.08	0.000
X ₁	-1.5126	0.2416	-6.261	1	99.10	99.10	99.100	39.20	0.000
X ₂ (mg L ⁻¹)	-4.4222	0.2416	-18.304	1	847.04	847.04	847.039	335.03	0.000
X ₃ (g)	1.0046	0.2416	4.158	1	43.71	43.71	43.713	17.29	0.000
X ₄ (% w/v)	1.5811	0.2416	6.544	1	108.27	108.27	108.274	42.83	0.000
X ₅ (μm)	-0.6175	0.2416	-2.556	1	16.51	16.51	16.514	6.53	0.017
X ₆ (rpm)	1.2256	0.2416	5.073	1	65.06	65.06	65.062	25.73	0.000
X ₁ * X ₁	0.0522	0.2064	0.253	1	0.59	0.16	0.162	0.06	0.802
X ₂ (mg L ⁻¹) * X ₂ (mg L ⁻¹)	-0.3897	0.2064	-1.889	1	7.97	9.02	9.018	3.57	0.071
X ₃ (g) * X ₃ (g)	-0.1104	0.2064	-0.535	1	0.48	0.72	0.724	0.29	0.597
X ₄ (% w/v) * X ₄ (% w/v)	0.0407	0.2064	0.197	1	0.26	0.10	0.098	0.04	0.845
X ₅ (μm) * X ₅ (μm)	-0.1794	0.2064	-0.869	1	1.63	1.91	1.910	0.76	0.393
X ₆ (rpm) * X ₆ (rpm)	-0.1970	0.2064	-0.955	1	2.31	2.31	2.305	0.91	0.349
X ₁ * X ₂ (mg L ⁻¹)	-1.1447	0.2811	-4.072	1	41.93	41.93	41.930	16.58	0.000
X ₁ * X ₃ (g)	0.1653	0.2811	0.588	1	0.87	0.87	0.875	0.35	0.562
X ₁ * X ₄ (% w/v)	-0.0347	0.2811	-0.123	1	0.04	0.04	0.039	0.02	0.903
X ₁ * X ₅ (μm)	-0.2172	0.2811	-0.773	1	1.51	1.51	1.509	0.60	0.447
X ₁ * X ₆ (rpm)	-0.3228	0.2811	-1.148	1	3.33	3.33	3.335	1.32	0.262
X ₂ (mg L ⁻¹) * X ₃ (g)	-0.3591	0.2811	-1.277	1	4.13	4.13	4.126	1.63	0.213
X ₂ (mg L ⁻¹) * X ₄ (% w/v)	0.7909	0.2811	2.814	1	20.02	20.02	20.019	7.92	0.009
X ₂ (mg L ⁻¹) * X ₅ (μm)	-0.4841	0.2811	-1.722	1	7.50	7.50	7.498	2.97	0.097
X ₂ (mg L ⁻¹) * X ₆ (rpm)	-0.3759	0.2811	-1.337	1	4.52	4.52	4.523	1.79	0.193
X ₃ (g) * X ₄ (% w/v)	0.2172	0.2811	0.773	1	1.51	1.51	1.509	0.60	0.447
X ₃ (g) * X ₅ (μm)	0.3972	0.2811	1.413	1	5.05	5.05	5.048	2.00	0.170
X ₃ (g) * X ₆ (rpm)	-0.2434	0.2811	-0.866	1	1.90	1.90	1.896	0.75	0.395
X ₄ (% w/v) * X ₅ (μm)	0.7222	0.2811	2.569	1	16.69	16.69	16.690	6.60	0.017
X ₄ (% w/v) * X ₆ (rpm)	0.0166	0.2811	0.059	1	0.01	0.01	0.009	0.00	0.953
X ₅ (μm) * X ₆ (rpm)	-0.1084	0.2811	-0.386	1	0.38	0.38	0.376	0.15	0.703
Residual error				25	63.21	63.21	2.528		
Lack-of-fit				17	62.91	62.91	3.701	101.19	0.000
Pure error				8	0.29	0.29	0.037		
Total				52	1365.53				

Regression coefficient $R^2 = 0.9537$, R^2 (Pred) = 0.7055, R^2 (adj) = 0.9037, $S = 1.59006$, PRESS = 402.082. Where SE, standard error of coefficient; DF, degree of freedom; Seq SS, sequential sum of squares; Adj SS, adjusted sum of squares; Adj MS, adjusted mean squares; PRESS, prediction residual error sum of squares; S, value of S chart.

over fitted model will not predict any new observations nearly as well as it fits the existing data. The term PRESS statistics is used to predict the responses of a new experiment and the smaller value of PRESS is more ideal [41]. The suitability of the model was evaluated by the residuals which is the difference between actual and the predicted response values. The lower value of RMSE (1.21) and AAD (1.17) yield best fit model equation. The ANOVA table shows the residual error, which measures the elements of variation in the response that cannot be explained by the model, and their occurrence in a normal distribution.

Fig. 9a shows that the observed residuals are plotted against the expected values, given by normal distribution.

It is a useful way to examine the hypothesis of normality of the observations. If the distribution of residuals is normal, the resulting diagram will be a straight line. It can be observed that the residuals from the analysis do not have any effect on the result and are the best residuals. If the correct model and hypotheses are fulfilled, the residuals must have a special relation to the other variables like the predicted response. Fig. 9b depicts the plot of residuals based on the predicted amounts of percentage decolorization. The residuals in this plot appear to be randomly scattered above and below the zero line. The greater spread of residuals in this plot signifies the increase in the fitted values. Fig. 9c shows the histogram of the residuals. A long tail in the plot

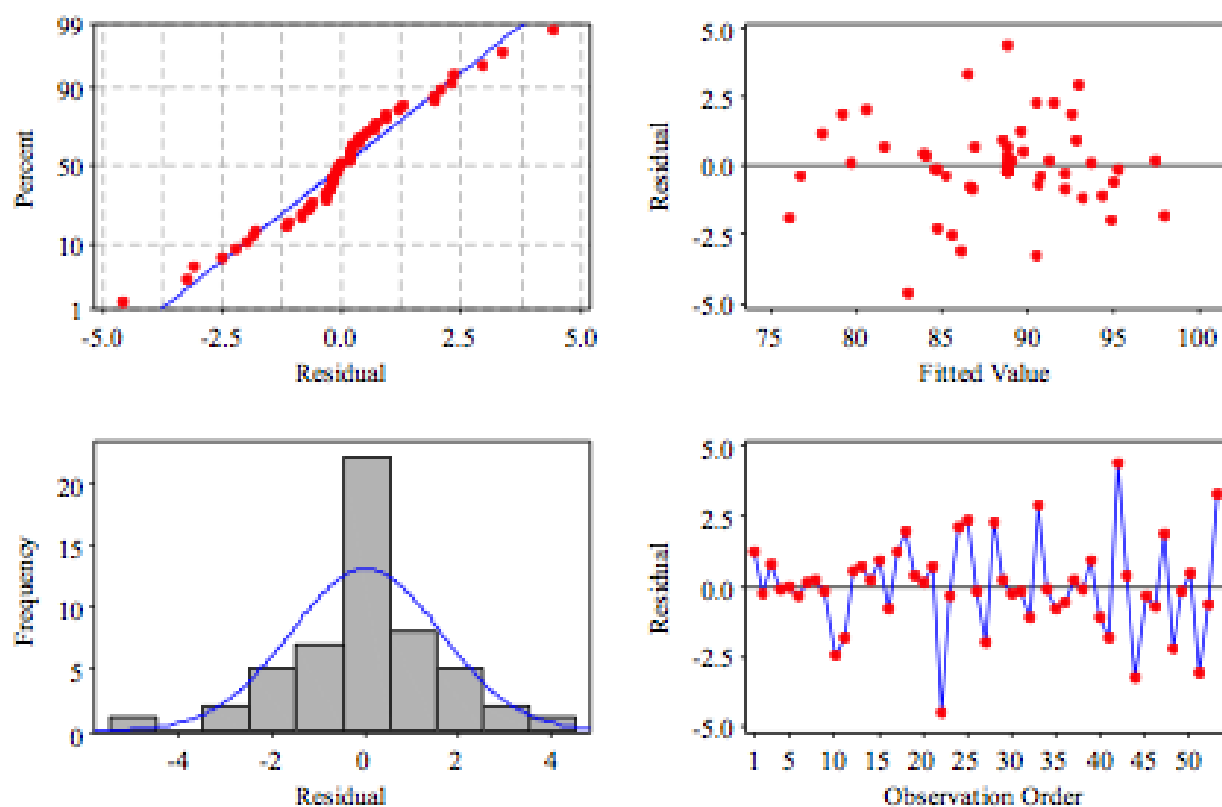


Fig. 9. Residual plots for CR color removal by LB-WB dual adsorbent. (a) Normal probability plot of residuals, (b) Residuals versus fitted values, (c) Frequency of observation versus residuals (d) Residuals versus the order of the data.

indicates the skewed distribution. The one or two bars that are far from the others may be outliers. The non-uniform bars in the plot represent the more fitted values. The chronological drawing data could be useful in the identification of residuals coordination. Fig. 9d illustrates the residuals in the order of corresponding observations. It was observed that the residuals in the plot fluctuate in a random pattern (chronological order) around the zero line in the order of observation, and this was used to determine the non-random error [41,54].

3.5.1 Contour and response surface plots

An elliptical shaped contour plot indicates the mutual interactions between the variables for percentage color removal of CR as shown in Figs. 10a–10d. The coordinates of the central point in each of these plot indicate the optimal value of the respective constituents. The central point is the point at which the slope of the contour is zero in all directions. The maximum predicted percentage decolorization is shown by the minimum curvature of the contour plot. Fig. 10a shows that the contour plot of percentage color removal CR as a function of initial dye concentration and initial pH. It occurs when the dye concentration ranges between 200 and 215 mg L⁻¹, pH in the range of 5.75–6.4, and the effect is insignificant. Fig. 10b shows that the maximum predicted response occurs when the initial dye concentration ranges between 200 and 215 mg L⁻¹ and the wheat bran dosage ranges from 1.25 to 1.75 g. Fig. 10c shows that the

maximum predicted yield occurs when the wheat bran dosage ranges between 1.625 and 1.75 g, and the live biomass dosage in the range of 2.875–3 % (w/v). Fig. 10d shows that the maximum predicted percentage decolorization occurs when the agitation speed ranges between 195 and 210 rpm and the wheat bran particle size ranges from 100 to 125 μ m, and the effect is not very significant.

The three-dimensional response surface plot was used to understand the main and interaction effects among the variables and to determine the maximum (optimum) response level of each variable. Response surface plots are developed as a function of two factors while maintaining all other factors at fixed levels. The optimum situations of the relative variables will resemble with the coordinates of the central point in the upmost level in each of these figures [41,55]. The response surface curves for percentage removal of CR are shown in Figs. 11a–11d. Fig. 11a shows the surface plot of the response variable as a function of initial pH and initial dye concentration. It clearly shows that the decolorization efficiency increased with the decrease in the pH and initial dye concentration. The value of pH in the range of 5.75–6.4 does not have significant effect, while a dye concentration ranges between 200 and 400 mg L⁻¹ has a significant effect on the decolorization of CR using LB-WB dual adsorbent. Fig. 11b shows that the increase in dye concentration, the less the decolorization efficiency, and more the wheat bran dosage, the better the removal efficiency. The response surface plot of wheat bran dosage ranges between 1.25 and 1.75 g does not have significant effect, while a dye concentra-

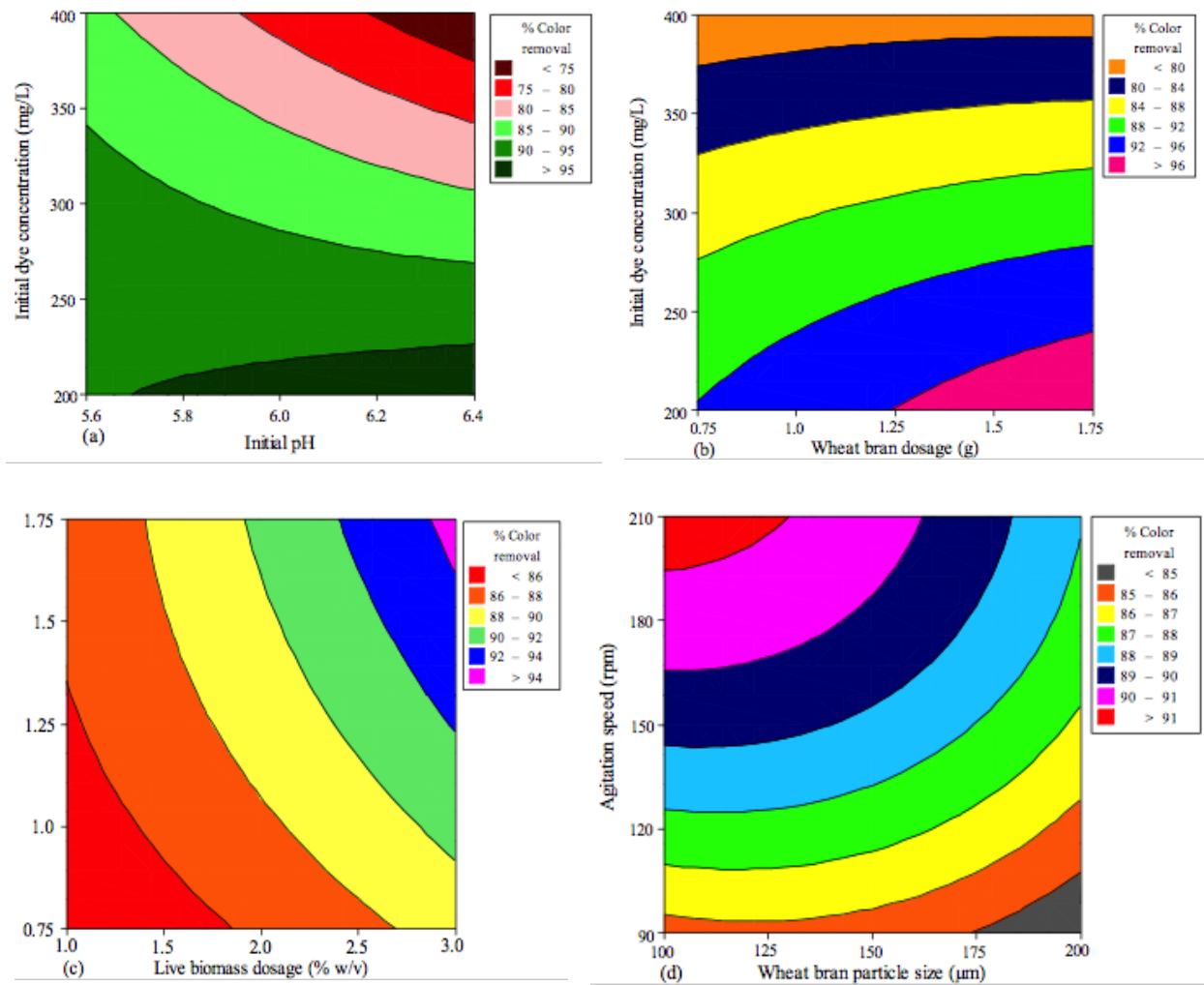


Fig. 10. Contour plots for interactive effect of (a) initial dye concentration and pH (b) initial dye concentration and wheat bran dosage (c) wheat bran dosage and live biomass dosage (d) agitation speed and wheat bran particle size.

tion in the range of 200–400 mg L⁻¹ shows a significant effect on color removal. Fig. 11c shows that the percentage color removal of CR increased with increase in live biomass dosage and decrease in wheat bran particle size. The response plot of live biomass dosage ranges between 1 and 3% (w/v) versus the wheat bran particle size in the range of 100–200 μm shows a significant effect on color removal. Similarly, Fig. 11d shows that with an increase in the agitation speed and decrease in wheat bran particle size, the decolorization efficiency improves. The response surface plot of wheat bran particle size in the range of 100–200 μm versus the agitation speed in the ranges between 90 and 210 rpm shows a significant effect on color removal of CR from aqueous solution. The optimal response values obtained from these plots are in close agreement with those values obtained from the experiment and regression model equation.

3.5.2 Process model validation

Three solutions with different values of ideal conditions were used to predict the optimum conditions for

CR dye decolorization by LB-WB dual adsorbent which is shown in Table 4. Experiments were done under fixed conditions and the results were compared to the predicted responses. The maximum color removal percentage (97.45%) was obtained in the experiment number 1, compared to the other two experiments. The optimal values of the process independent variables for maximal percentage of CR color removal are given in Table 5. The comparison between actual and predicted responses shows a good relation between them, and it suggests that the empirical model resulted from the design could as well be used for describing the relation between factors and the response in CR dye decolorization.

3.6. Comparison of decolorization efficiency between individual adsorbents and LB-WB dual adsorbent

The batch experiments for the removal of CR color were carried out with individual adsorbents and dual adsorbent in separate batches for comparison purpose. The initial CR dye concentration was fixed as 300 mg L⁻¹ and was treated

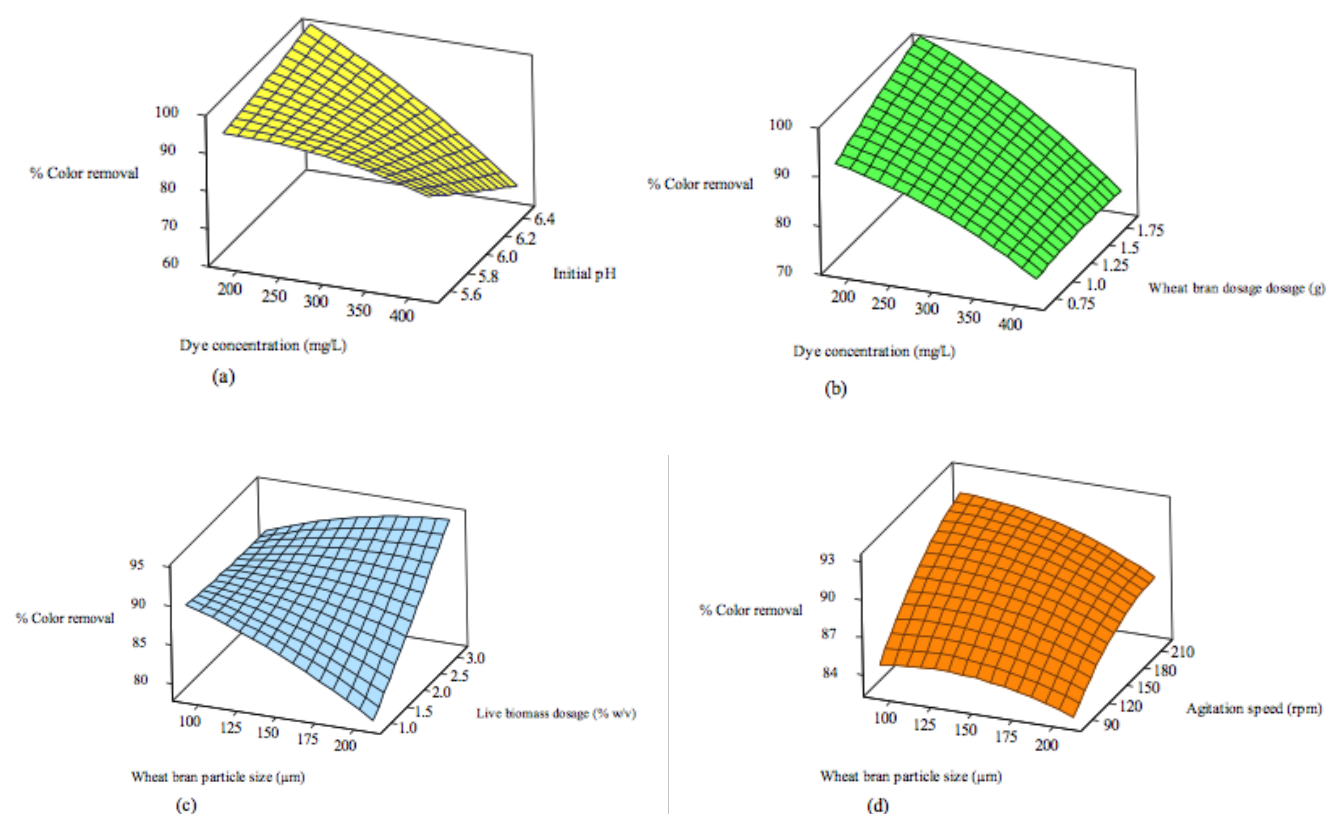


Fig. 11. Surface plots for interactive effect of (a) initial pH and dye concentration (b) wheat bran dosage and initial dye concentration (c) live biomass dosage and wheat bran particle size (d) agitation speed and wheat bran particle size.

Table 4
Validation of process model

Expt.	Process conditions						CR color removal (%)	
	X_1	X_2 (mg L ⁻¹)	X_3 (g)	X_4 (% w/v)	X_5 (μm)	X_6 (rpm)	Actual value	Predicted value
1	6	200	1.25	2	150	150	97.45	98.24
2	5.8	250	1.5	2.5	125	120	92.56	94.62
3	6	300	1.25	2	150	150	88.57	90.36

Table 5
Optimal values of the process independent variables for maximum percentage color removal of Congo red dye

Process parameters	Optimum value	CR color removal (%)
Initial pH (X_1)	6	97.45
Initial dye concentration, mg L ⁻¹ (X_2)	200	
Wheat bran dosage, g (X_3)	1.25	
Live biomass dosage, % w/v (X_4)	2	
Wheat bran particle size, μm (X_5)	150	
Agitation speed, rpm (X_6)	150	

with 32.5 g L⁻¹ of wheat bran and *Neurospora crassa* live biomass in separate batches. The percentage color removal was calculated for regular time intervals and compared with the decolorization efficiency of the dual adsorbent (12.5 g L⁻¹ of

wheat bran and 20 g L⁻¹ of *Neurospora crassa* live biomass). The results were shown in Fig. 12 and was observed that the dual adsorbent had better decolorization efficiency when compared to the individual adsorbents.

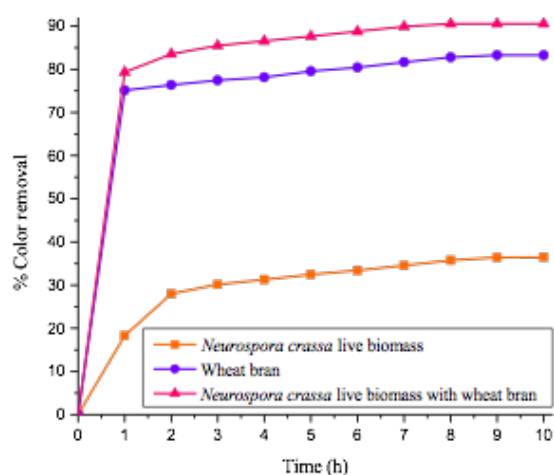


Fig. 12. Comparison of percentage color removal between individual adsorbents and LB-WB dual adsorbent.

(Initial pH: 6; initial dye concentration: 300 mg L⁻¹; LB-WB dual adsorbent dosage: 32.5 g L⁻¹ (wheat bran dosage 12.5 g and live biomass dosage 20 g); wheat bran dosage: 32.5 g L⁻¹; live biomass dosage: 32.5 g L⁻¹; wheat bran particle size: <100 μm; agitation speed: 150 rpm; temperature: 303 K; contact time 10 h).

4. Conclusion

The present study clearly demonstrated the applicability of a dual adsorbent consisting of live fungal biomass of *Neurospora crassa* and wheat bran for the removal of CR color from an aqueous solution. In addition, the fungus used was nonpathogenic. The adsorption was found to be strongly dependent on initial pH, initial dye concentration, wheat bran dosage, live biomass dosage, wheat bran particle size, and agitation speed. Under optimal values of process parameters, effective adsorption (decolorization) of CR was determined. This study clearly showed that response surface methodology was one of the suitable methods to optimize the best operating conditions to maximize the color removal. The predicted response values fitted well with the actual values ($R^2 = 0.9537$, RMSE = 1.21, and AAD = 1.17). Analysis of variance confirms the accuracy of the model by using larger value of F, lower value of P, non-significant lack of fit, and the maximum value of regression coefficient. A removal percentage of 97.45% was attained, which was good compared to the predicted value 98.24% using regression model equation. This shows that the quadratic model properly explains the influence of the chosen variables on CR color removal by the dual adsorbent system. The effect of other factors such as electrolytes, surfactants, temperature, and mixture of dyes were also studied. Comparison of decolorization efficiency between individual adsorbents and dual adsorbent resulted in the findings that the dual adsorbent had better decolorization efficiency. It was concluded from the results the LB-WB dual adsorbent as a promising adsorbent for effective decolorization of anionic dyes from industrial effluents.

Symbols and abbreviations

AAD — Absolute average deviation
Adj MS — Adjusted mean squares

Adj SS	—	Adjusted sum of squares
AG	—	Acid green
ANOVA	—	Analysis of variance
BET	—	Brunauer–Emmett–Teller
CCD	—	Central composite design
COD	—	Chemical oxygen demand (mg L ⁻¹)
CR	—	Congo red dye
CTAB	—	Cetyltrimethylammonium bromide
C _o	—	Initial dye concentration in solution (mg L ⁻¹)
C _t	—	Dye concentration in solution at any time t (mg L ⁻¹)
CV	—	Coomassie violet
DF	—	Degree of freedom
F	—	Fisher's 'F'-test
f	—	Number of variables
MTCC	—	Microbial type culture collection
N	—	Numbers of experimental runs
N _o	—	Center points
P	—	Probability value
PRESS	—	Predicted residual error sum of squares
R ²	—	Linear regression correlation coefficient
RBBR	—	Remazol brilliant blue R
RMSE	—	Root mean square error
RSM	—	Response surface methodology
S	—	Value of S chart
SD	—	Standard deviation
SDS	—	Sodium dodecylbenzenesulfonate
SE	—	Standard error
Seq SS	—	Sequential sum of squares
T _{statistics}	—	Student 'T'-test
x _i	—	Dimensionless value of a process variable X _i
X _i	—	Real value of an independent variable
X _o	—	Value of X _i at the center point
X ₁	—	Initial pH of the dye solution
X ₂	—	Initial dye concentration (mg L ⁻¹)
X ₃	—	Wheat bran dosage (g)
X ₄	—	Live biomass dosage (g)
X ₅	—	Wheat bran particle size (μm)
X ₆	—	Agitation speed (rpm)
Y	—	Predicted response variable of percentage decolorization
y _a	—	Actual response variable of percentage decolorization
2 ^f	—	Number of factorial points
2f	—	Axial points

Greek letters

β ₀	—	Offset term
β _i	—	Regression coefficients for linear effect
β _{ii}	—	Regression coefficients for quadratic effect
β _{ij}	—	Regression coefficients for interaction effect
δX	—	Step change
λ _{max}	—	Maximum wavelength of CR dye (nm)

References

- [1] R. Malarvizhi, N. Sulochana, Sorption isotherm and kinetic studies of methylene blue uptake onto activated carbon prepared from wood apple shell, J. Environ. Prot. Sci., 2 (2008) 40–46.

- [2] S.L. Chan, Y.P. Tan, A.H. Abdullah, S.T. Ong, Equilibrium, kinetic and thermodynamic studies of a new potential biosorbent for the removal of basic blue 3 and congo red dyes: Pineapple (*Ananas comosus*) plant stem, *J. Taiwan Inst. Chem. Eng.*, 61 (2016) 306–315.
- [3] V.S. Mane, P.V. Vijay Babu, Kinetic and equilibrium studies on the removal of congo red from aqueous solution using *Eucalyptus* wood (*Eucalyptus globulus*) saw dust, *J. Taiwan Inst. Chem. Eng.*, 44 (2013) 81–88.
- [4] A.R. Cestari, E.F.S. Vieira, G.S. Vieira, L.E. Almeida, Aggregation and adsorption of reactive dyes in the presence of an anionic surfactant on mesoporous aminopropyl silica, *J. Colloid Interface Sci.*, 309 (2007) 402–411.
- [5] S.R. Couto, Dye removal by immobilized fungi, *Biotechnol. Adv.*, 27 (2009) 227–235.
- [6] R.K. Gautam, V. Rawat, S. Banerjee, M.A. Sanroman, S. Soni, S. K. Singh, M.C. Chattopadhyaya, Synthesis of bimetallic Fe–Zn nanoparticles and its application towards adsorptive removal of carcinogenic dye malachite green and congo red in water, *J. Mol. Liq.*, 212 (2015) 227–236.
- [7] N. Chaukura, B.B. Mamba, S.B. Mishra, Conversion of post consumer waste polystyrene into a high value adsorbent and its sorptive properties for congo red removal from aqueous solution, *J. Environ. Manage.*, 193 (2017) 280–289.
- [8] G.C. Panda, S.K. Das, A.K. Guha, Jute stick powder as a potential biomass for the removal of congo red and rhodamine B from their aqueous solution, *J. Hazard. Mater.*, 164 (2009) 374–379.
- [9] A. Mittal, J. Mittal, A. Malviya, V.K. Gupta, Adsorptive removal of hazardous anionic dye congo red from wastewater using waste materials and recovery by desorption, *J. Colloid Interface Sci.*, 340 (2009) 16–26.
- [10] C. Srilakshmi, R. Saraf, Ag-doped hydroxyapatite as efficient adsorbent for removal of congo red dye from aqueous solutions: synthesis, kinetic and equilibrium adsorption isotherm analysis, *Microporous Mesoporous Mater.*, 219 (2016) 134–144.
- [11] C. Xia, Y. Jing, Y. Jia, D. Yue, J. Ma, X. Yin, Adsorption properties of congo red from aqueous solution on modified hectorite: Kinetic and thermodynamic studies, *Desalination*, 265 (2011) 81–87.
- [12] V.K. Gupta, Suhas, Application of low-cost adsorbents for dye removal – A review, *J. Environ. Manage.*, 90 (2009) 2313–2342.
- [13] G. Crini, Non-conventional low cost adsorbents for dye removal: a review, *Bioresour. Technol.*, 97 (2006) 1061–1085.
- [14] A. Srinivasn, T. Viraraghavan, Decolorization of dye wastewaters by biosorbents: A review, *J. Environ. Manage.*, 91 (2010) 1915–1929.
- [15] X. Han, W. Wang, X. Ma, Adsorption characteristics of methylene blue onto low cost biomass material lotus leaf, *Chem. Eng. J.*, 171 (2011) 1–8.
- [16] D. Pathania, A. Sharma, Z.M. Siddiqi, Removal of congo red dye from aqueous system using *Phoenix dactylifera* seeds, *J. Mol. Liq.*, 219 (2016) 359–367.
- [17] E. Khan, M. Li, C.P. Huang, Hazardous waste treatment technologies, *Water Environ. Res.*, 55 (2008) 1654–1708.
- [18] A. Afkhami, M. Saber-Tehrani, H. Bagheri, Modified maghemite nanoparticles as an efficient adsorbent for removing some cationic dyes from aqueous solution, *Desalination*, 263 (2010) 240–248.
- [19] F. Deniz, S. Karaman, Removal of Basic Red 46 dye from aqueous solution by pine tree leaves, *Chem. Eng. J.*, 170 (2011) 67–74.
- [20] Z. Hu, H. Chen, F. Ji, S. Yuan, Removal of congo red from aqueous solution by cattail root, *J. Hazard. Mater.*, 173 (2010) 292–297.
- [21] G. Sun, X. Xu, Sunflower stalks as adsorbents for color removal from textile wastewater, *Ind. Eng. Chem. Res.*, 36 (1997) 808–812.
- [22] N.A. Oladoja, C.O. Aboluwoye, Y.B. Oladimeji, A.O. Ashogbon, I.O. Otemuyiwa, Studies on castor seed shell as a sorbent in basic dye contaminated wastewater remediation, *Desalination*, 227 (2008) 190–203.
- [23] M. Arami, N.Y. Limaee, N.M. Mahmoodi, N.S. Tabrizi, Equilibrium and kinetics studies for the adsorption of direct and acid dyes from aqueous solution by soy meal hull, *J. Hazard. Mater.*, B135 (2006) 171–179.
- [24] M.T. Sulak, E. Demirbas, M. Kobya, Removal of astrazon yellow 7GL from aqueous solutions by adsorption onto wheat bran, *Bioresour. Technol.*, 98 (2007) 2590–2598.
- [25] Y. Fu, T. Viraraghavan, Fungal decolorization of dye wastewaters: A review, *Bioresour. Technol.*, 79 (2001) 251–262.
- [26] N.K. Pazarlioglu, R.O. Urek, F. Ergun, Biodecolourization of direct blue 15 by immobilized *Phanerochaete chrysosporium*, *Process Biochem.*, 40 (2005) 1923–1929.
- [27] G. Palmieri, G. Cennamo, G. Sannia, Remazol brilliant blue R decolourisation by the fungus *Pleurotus ostreatus* and its oxidative enzymatic system, *Enzyme Microb. Technol.*, 36 (2005) 17–24.
- [28] S.K. Das, J. Bhowal, A.R. Das, A.K. Guha, Adsorption behavior of rhodamine B on *Rhizopus oryzae* biomass, *Langmuir*, 22 (2006) 7265–7272.
- [29] C. Novotny, B. Rawal, M. Bhatt, M. Patel, V. Sasek, H.P. Molitoris, Capacity of *Irpex lacteus* and *Pleurotus ostreatus* for decolorization of chemically different dyes, *J. Biotechnol.*, 89 (2001) 113–122.
- [30] C. Park, M. Lee, B. Lee, S.W. Kim, H.A. Chase, J. Lee, S. Kim, Biodegradation and biosorption for decolorization of synthetic dyes by *Funalia trogii*, *Biochem. Eng. J.*, 36 (2007) 59–65.
- [31] P. Vairavel, V. Ramachandra Murty, S. Nethaji, Removal of congo red dye from aqueous solutions by adsorption onto a dual adsorbent (*Neurospora crassa* dead biomass and wheat bran): optimization, isotherm, and kinetics studies, *Desal. Water Treat.*, 68 (2017) 274–292.
- [32] A.A. Kadam, H.S. Lade, S.M. Patil, S.P. Govindwar, Low cost CaCl₂ pretreatment of sugarcane bagasse for enhancement of textile dyes adsorption and subsequent biodegradation of adsorbed dyes under solid state fermentation, *Bioresour. Technol.*, 132 (2013) 276–284.
- [33] T. Akar, T.A. Demir, I. Kiran, A. Ozcan, A.S. Ozcan, S. Tunali, Biosorption potential of *Neurospora crassa* cells for decolorization of acid red 57 dye, *J. Chem. Technol. Biotechnol.*, 81 (2006) 1100–1106.
- [34] I. Kiran, T. Akar, S. Tunali, Biosorption of Pb(II) and Cu(II) from aqueous solutions by pretreated biomass of *Neurospora crassa*, *Process Biochem.*, 40 (2005) 3550–3558.
- [35] V. Vadevelan, K. Vasanth Kumar, Equilibrium, kinetics, mechanism, and process design for the sorption of methylene blue onto rice husk, *J. Colloid Interface Sci.*, 286 (2005) 90–100.
- [36] X.S. Wang, J.P. Chen, Biosorption of congo red from aqueous solution using wheat bran and rice bran: Batch studies, *Sep. Sci. Technol.*, 44 (2009) 1452–1466.
- [37] S. Nethaji, A. Sivasamy, G. Thennarasu, S. Saravanan, Adsorption of malachite green dye onto activated carbon derived from *Borassus aethiopum* flower biomass, *J. Hazard. Mater.*, 181 (2010) 271–280.
- [38] B. Zhang, X. Han, P. Gu, S. Fang, J. Bai, Response surface methodology approach for optimization of ciprofloxacin adsorption using activated carbon derived from the residue of desiccated rice husk, *J. Mol. Liq.*, 238 (2017) 316–325.
- [39] A. Asfaram, M. Ghaedi, S. Hajati, A. Goudarzi, A.A. Bazrafshan, Simultaneous ultrasound assisted ternary adsorption of dyes onto copper-doped zinc sulfide nanoparticles loaded on activated carbon: Optimization by response surface methodology, *Spectrochim. Acta Mol. Biomol. Spectrosc.*, 145 (2015) 203–212.
- [40] K. Ravikumar, K. Pakshirajan, T. Swaminathan, K. Balu, Optimization of batch process parameters using response surface methodology for dye removal by a novel adsorbent, *Chem. Eng. J.*, 105 (2005) 131–138.
- [41] M.R. Sohrabi, S. Amiri, H.R.F. Masoumi, M. Moghri, Optimization of direct yellow 12 dye removal by nanoscale zero-valent iron using response surface methodology, *J. Ind. Eng. Chem.*, 20 (2014) 2535–2542.

- [42] F.A. Pavan, Y. Gushikem, A.C. Mazzocato, S.L.P. Dias, E.C. Lima, Statistical design of experiments as a tool for optimizing the batch conditions to methylene blue biosorption on yellow passion fruit and mandarin peels, *Dyes Pigm.*, 72 (2007) 256–266.
- [43] M.C. Somasekhara Reddy, Removal of direct dye from aqueous solutions with an adsorbent made from tamarind fruit shell, an agricultural solid waste, *J. Sci. Ind. Res.*, 65 (2006) 443–446.
- [44] V.S. Munagapati, D.S. Kim, Adsorption of anionic azo dye congo Red from aqueous solution by cationic modified orange peel powder, *J. Mol. Liq.*, 220 (2016) 540–548.
- [45] N.K. Amin, Removal of reactive dye from aqueous solutions by adsorption onto activated carbons prepared from sugarcane bagasse pith, *Desalination*, 223 (2008) 152–161.
- [46] K.K. Wong, C.K. Lee, K.S. Low, M.J. Haron, Removal of Cu and Pb by tartaric acid modified rice husk from aqueous solutions, *Chemosphere*, 50 (2003) 23–28.
- [47] E. Errais, J. Duplay, F. Darragi, I.M. Rabet, A. Aubert, F. Huber, G. Morvan, Efficient anionic dye adsorption on natural untreated clay: Kinetic study and thermodynamic parameters, *Desalination*, 275 (2011) 74–81.
- [48] B.H. Hameed, A.A. Ahmad, N. Aziz, Isotherms, kinetics and thermodynamics of acid dye adsorption on activated palm ash, *Chem. Eng. J.*, 133 (2007) 195–203.
- [49] I.A.W. Tan, B.H. Hameed, A.L. Ahmad, Equilibrium and kinetic studies on basic dye adsorption by oil palm fibre activated carbon, *Chem. Eng. J.*, 127 (2007) 111–119.
- [50] A. Sivasamy, S. Nethaji, J.L. Nisha, Equilibrium, kinetic and thermodynamic studies on the biosorption of reactive acid dye on *Enteromorpha flexuosa* and *Gracilaria corticata*, *Environ. Sci. Pollut. Res.*, 19 (2012) 1687–1695.
- [51] N.S. Maurya, A.K. Mittal, P. Cornel, E. Rother, Biosorption of dyes using dead macro fungi: Effect of dye structure, ionic strength and pH, *Bioresour. Technol.*, 97 (2006) 512–521.
- [52] Y.S. Al-Degs, M.I. El-Barghouthi, A.H. El-Sheikh, G.M. Walker, Effect of solution pH, ionic strength, and temperature on adsorption behavior of reactive dyes on activated carbon, *Dyes Pigm.*, 77 (2008) 16–23.
- [53] G. Alberghina, R. Bianchini, M. Fichera, S. Fisichella, Dimerization of cibacron blue F3GA and other dyes: Influence of salts and temperature, *Dyes Pigm.*, 46 (2000) 129–137.
- [54] M.B. Kasiri, A.R. Khataee, Photooxidative decolorization of two organic dyes with different chemical structures by UV/H₂O₂ process: Experimental design, *Desalination*, 270 (2011) 151–159.
- [55] P. Muthamilselvi, R. Karthikeyan, B.S.M. Kumar, Adsorption of phenol onto garlic peel: optimization, kinetics, isotherm, and thermodynamic studies, *Desal. Water Treat.*, 57 (2016) 2089–2103.

Supplementary materials

Optimization of batch process parameters for Congo red color removal by *Neurospora crassa* live fungal biomass with wheat bran dual adsorbent using response surface methodology

1. Introduction

The optimization of all those variables using the univariate procedure is very tedious, because by varying just one factor by the time; other parameter were kept at a constant level. This procedure does not study the interactive effects among the variables, so the best condition could not be attained. The approach has more number of experiments, which is not economical and is also time-consuming. In order to overcome the disadvantages in the univariate procedure, multivariate statistical design of experiments can be carried out to achieve the best optimization of the system. Response surface methodology utilizes the polynomial equation to describe the behavior of experimental data. The objective of the response surface method is to optimize the levels of variables [1].

2. Materials and methods

2.1 Factorial experimental design

Factorial experimental design is used to study the effects of several factors on optimization of a particular process. It also determines factors which have important effects on a response as well as how the effect of each factor varies with the level of the other factors. The linear, quadratic, and interactions effects of process factors on the response were studied with the help of the empirical model developed using RSM [2]. Response surface methods are used to [3]

- a) find factor settings (operating conditions) that produce the best response;

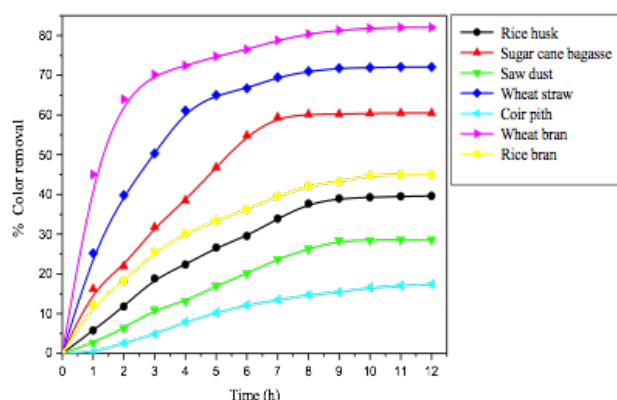


Fig. S1. Selection of suitable agricultural by-product for the removal of CR dye. (Initial pH: 6; Initial dye concentration: 100 mg L⁻¹; adsorbent dosage: 5 g L⁻¹; adsorbent particle size: <100 μm; agitation speed: 150 rpm; temperature: 303 K; contact time 12 h).

- b) find factor settings that satisfy operating or process specifications;
c) examine the relationship between response variable and a set of quantitative experimental factors.

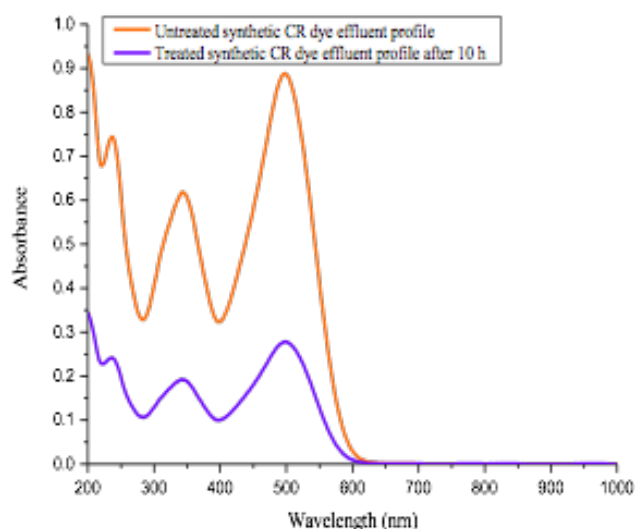


Fig. S2. Synthetic CR dye effluent decolorization profile obtained in batch studies at 10 h using LB-WB dual adsorbent compared with untreated effluent profile. (Initial pH: 6; Initial dye concentration: 200 mg L⁻¹; wheat bran dosage: 10 g L⁻¹; live biomass dosage: 1.5% (w/v); wheat bran particle size: <100 μm; agitation speed: 150 rpm; temperature: 303 K; contact time 10 h)

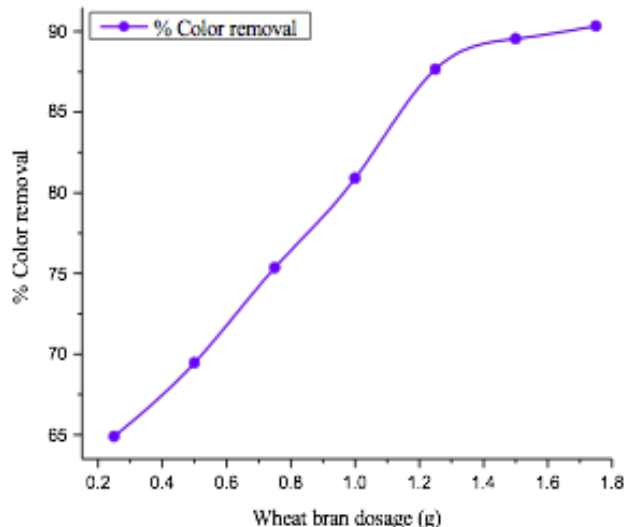


Fig.S3. Effect of wheat bran dosage on CR color removal by LB-WB dual adsorbent. (Initial pH: 6; Initial dye concentration: 300 mg L⁻¹; live biomass dosage: 1.5% (w/v); wheat bran particle size: <100 μm; agitation speed: 150 rpm; temperature: 303 K; contact time 10 h).

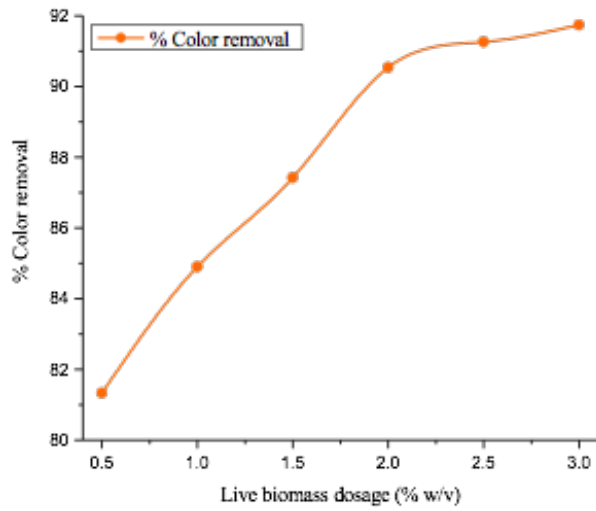


Fig. S4. Effect of live biomass dosage on CR color removal by LB-WB dual adsorbent. (Initial pH: 6; initial dye concentration: 300 mg L⁻¹; wheat bran dosage: 12.5 g L⁻¹; wheat bran particle size: <100 μm; agitation speed: 150 rpm; temperature: 303 K; contact time 10 h).

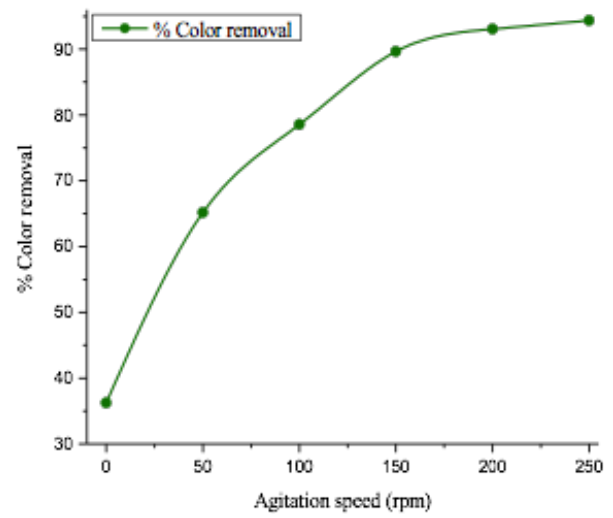


Fig. S6. Effect of agitation speed on CR color removal by LB-WB dual adsorbent. (Initial pH: 6; initial dye concentration: 300 mg L⁻¹; wheat bran dosage: 12.5 g L⁻¹; live biomass dosage: 2% (w/v); wheat bran particle size: <100 μm; temperature: 303 K; contact time 10 h).

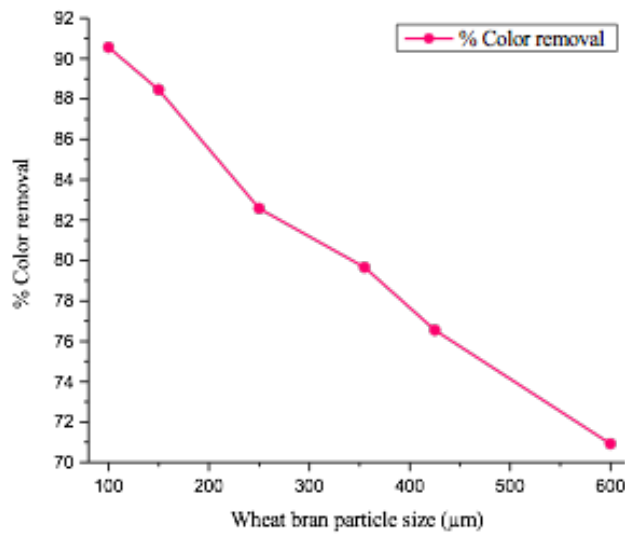


Fig. S5. Effect of wheat bran particle size on CR color removal by LB-WB dual adsorbent. (Initial pH: 6; initial dye concentration: 300 mg L⁻¹; wheat bran dosage: 12.5 g L⁻¹; live biomass dosage: 2% (w/v); agitation speed: 150 rpm; temperature: 303 K; contact time 10 h).

References for supplementary materials

- [1] M.R. Sohrabi, S. Amiri, H.R.F. Masoumi, M. Moghri, Optimization of direct yellow 12 dye removal by nanoscale zero-valent iron using response surface methodology, *J. Ind. Eng. Chem.*, 20 (2014) 2535–2542.
- [2] F.A. Pavan, Y. Gushikem, A.C. Mazzocato, S.L.P. Dias, E.C. Lima, Statistical design of experiments as a tool for optimizing the batch conditions to methylene blue biosorption on yellow passion fruit and mandarin peels, *Dyes Pigm.*, 72 (2007) 256–266.
- [3] D.C. Montgomery, G.C. Runger, *Applied statistics and probability for engineers*, 5th ed., John Wiley & Sons, 2011.